

文章编号: 0253-2409(2014)03-0350-07

# Production of dimethylether (DME) as a clean fuel using sonochemically prepared CuO and/or ZnO-modified $\gamma$ -alumina catalysts

Sameh M. K. Aboul-Fotouh

(Ain Shams University, Faculty of Education, Chemistry Department, Roxy, Cairo 11566, Egypt)

**Abstract:** The catalytic conversion of methanol to dimethylether (DME) was studied over CuO/Al<sub>2</sub>O<sub>3</sub>, ZnO/Al<sub>2</sub>O<sub>3</sub> and ZnO-CuO/Al<sub>2</sub>O<sub>3</sub> nanocatalysts prepared in presence or absence of ultrasonic irradiation. The catalysts were characterized by X-ray diffraction (XRD), surface characterization method (BET), scanning electron microscope (SEM), H<sub>2</sub>-temperature programmed reduction (H<sub>2</sub>-TPR) and temperature programmed desorption of ammonia (NH<sub>3</sub>-TPD). The experimental results show that during catalytic dehydration of methanol to dimethylether, the activities of the CuO/Al<sub>2</sub>O<sub>3</sub>, ZnO/Al<sub>2</sub>O<sub>3</sub> and ZnO-CuO/Al<sub>2</sub>O<sub>3</sub> catalysts prepared using ultrasonic treatment are much higher than those prepared in absence of ultrasonication. SEM shows that the use of ultrasonication results in much smaller nanoparticles. BET and XRD show that the ultrasonication increases the surface area and pore volume of the catalysts. H<sub>2</sub>-TPR profiles indicated that reducibility of the sonicated nanocatalysts is carried out at lower temperatures. NH<sub>3</sub>-TPD shows that ultrasound irradiation has enhanced the acidity of the nanocatalyst and hence enhanced catalytic performance for DME formation.

**Keywords:** ultrasonication; methanol; DME;  $\gamma$ -Al<sub>2</sub>O<sub>3</sub>; CuO; ZnO

**CLC number:** O643 **Document code:** A

Dimethyl ether (DME) has been found to be an alternative diesel fuel because it has low NO<sub>x</sub> emission, near-zero smoke amounts and less engine noise compared with traditional diesel fuels<sup>[1,2]</sup>. It can also be used to replace chlorofluorocarbons (CFCs) which destroy ozone layer of the atmosphere and used as an intermediate for producing many valuable chemicals such as lower olefins, methyl acetate, dimethyl sulfate and liquefied petroleum gas (LPG) alternative. It is also used in power generation and as an aerosol propellant, such as in hair spray and shaving cream, due to its liquefaction property<sup>[3-7]</sup>. Hence, there is a growing demand to produce a large amount of DME to meet the global need.

Dimethyl ether can be produced by methanol dehydration over a solid-acid catalyst or direct synthesis from syngas by employing a hybrid catalyst, comprising a methanol synthesis component and a solid-acid catalyst<sup>[8]</sup>. Methanol dehydration to dimethyl ether is a potentially important process and more favorable in the views of thermodynamics and economy<sup>[9]</sup>. Commercially,  $\gamma$ -Al<sub>2</sub>O<sub>3</sub> is used as the catalyst for this reaction. It has high surface area, excellent thermal stability, high mechanical resistance and catalytic activity for DME formation due to its surface acidity. Recently, many methods have been

applied to synthesize alumina with a higher specific surface area and activity for DME synthesis<sup>[10]</sup>.

CuO/ZnO/Al<sub>2</sub>O<sub>3</sub> catalysts have been widely used in methanol and DME synthesis from CO hydrogenation because of their high catalytic activity, long lifetime, high poison resistance, and relatively low reaction temperature and pressure<sup>[11-16]</sup>. In spite of the wide use of these catalysts, novel technologies such as ultrasound energy application on catalytic performance of CuO/ZnO/Al<sub>2</sub>O<sub>3</sub> catalysts is still not well understood and examined.

Aboul-Fotouh<sup>[17]</sup> have found that ultrasound irradiation can enhance and improve the catalytic performance of halogenated  $\gamma$ -Al<sub>2</sub>O<sub>3</sub> catalyst. Therefore, the purpose of the current research is to investigate the effect of ultrasound irradiation on the preparation of CuO, ZnO and ZnO-CuO supported on  $\gamma$ -Al<sub>2</sub>O<sub>3</sub> nano-catalysts. The surface characterization and acidity of the catalysts were investigated to acquire an insight on the relationship between characterization and activity of these catalysts for the dehydration of methanol to dimethylether (DME).

## 1 Experimental

### 1.1 Preparation of the catalysts

The powdered  $\gamma$ -Al<sub>2</sub>O<sub>3</sub> was doped with an aqueous solution of copper nitrate and /or zinc nitrate

**Received date:** 2013-12-18; **Received in revised form:** 2014-01-30.

**Corresponding author:** samehaboufotouh@yahoo.com.

**Current address:** Northern Border University, Faculty of Science, Chemistry Department, Kingdom of Saudi Arabia.

本文的英文电子版由 Elsevier 出版社在 ScienceDirect 上出版 (<http://www.sciencedirect.com/science/journal/18725813>)。

containing the requisite quantity to obtain 3.0% CuO and/or ZnO (by weight). These catalysts were subjected to ultrasonic irradiation during the impregnation step using Ultrasonic Processor UP50H (Hielscher) with a titanium sonotrode  $S_3$  and having a tip diameter of 3 mm, with 50 W/cm<sup>2</sup> power intensity (related to 100% amplitude setting). The ultrasonic irradiation lasted for 1 h at 25 °C, followed by centrifugation for 30 min. The catalysts were dried at 110 °C overnight and calcined at 400 °C for 2 h in air flow. The ultrasonicated catalysts were defined as CuO/Al<sub>2</sub>O<sub>3</sub> (U), ZnO/Al<sub>2</sub>O<sub>3</sub> (U) and ZnO-CuO/Al<sub>2</sub>O<sub>3</sub> (U). For comparison, a conventionally impregnated catalyst was similarly prepared except that the ultrasonic irradiation was replaced by stirring of the catalysts during the impregnation of CuO and/or ZnO on alumina at room temperature. The catalysts were dried and calcined as above. In absence of ultrasonication the catalysts were defined as CuO/Al<sub>2</sub>O<sub>3</sub>, ZnO/Al<sub>2</sub>O<sub>3</sub> and ZnO-CuO/Al<sub>2</sub>O<sub>3</sub>.

## 1.2 Hydroconversion reactor system and reaction product analysis

A silica glass flow-type tubular reactor system loaded with 0.1 g of the current catalyst was used. The reactor was heated in an insulated wider silica tube jacket, thermostated to  $\pm 1$  °C. Argon was used as a carrier gas at a flow rate of 30 cm<sup>3</sup>/min in all runs. The methanol feed was introduced into the reactor via continuous evaporation applying argon flow passing into a closed jar thermostated at a fixed temperature of 26 °C, whereby the quantity of methanol was always  $4.98 \times 10^{-2}$  mol/h. The reaction runs were investigated at temperatures ranging between 200 ~ 400 °C, with 25 °C increments. The reaction effluent was analyzed using a Perkin-Elmer Autosystem XL gas-chromatograph with a 4 m long column, packed with 10% squalane plus 10% didecyl phthalate supported on Chromosorb W-HP of 80 ~ 100 mesh. A flame ionization detector and a Totalchrom Navigator Programme computed were used.

## 1.3 Temperature programmed desorption (TPD) of ammonia

The procedure adopted by Aboul-Gheit<sup>[18,19]</sup> using Differential Scanning Calorimetry (DSC) was applied for detecting and evaluating presorbed ammonia from the acid sites of a catalyst. Ammonia presorption was initially carried out in a silica-tube furnace as follows; after evacuation of the catalyst at  $1.33 \times 10^{-3}$  Pa whilst heating for 30 min at 500 °C and subsequent cooling under vacuum to 50 °C, ammonia was introduced through the catalyst at a flow-rate of 50 cm<sup>3</sup>/min till saturation, normally 15 min. The

samples were then run in DSC unit (Mettler TA-3000) using standard aluminum crucibles in a continuous current of ultra-pure N<sub>2</sub> gas at a flow-rate of 30 cm<sup>3</sup>/min. The heating rate was 20 K/min and the full-scale range was 25 mW. The thermograms obtained for all samples show two peaks; a low-temperature peak corresponding to the ammonia desorption enthalpy from the weak acid sites of the catalyst ( $\Delta H_d$ ) and a high temperature peak corresponding to the ammonia desorption enthalpy ( $\Delta H_d$ ) from the strong acid sites. The  $\Delta H_d$  values were proportional to the number of acid sites, whereas the peak temperature ( $T_{max}$ ) was taken to correlate the acid sites strength of the catalysts; the higher the  $T_{max}$  value, the stronger the acid sites in the catalyst.

## 1.4 X-ray diffraction patterns of the catalysts

The X-ray diffraction patterns of the catalysts under study were carried out using a Phillips X, Pert Diffractometer PW 1390 at 40 kV and 30 mA with Ni Filter and Cu  $K\alpha$  radiation. The XRD runs were carried out up to  $2\theta$  of 60°. The traditional XRD patterns obtained for the current catalysts show more or less similar  $2\theta$  of the diffraction peaks.

## 1.5 Scanning electron microscope (SEM)

The SEM samples were mounted on aluminum slabs and sputter-coated with a thin gold layer of ~ 15 nm thickness using an Edward sputter-coater. The samples were then examined in a scanning electron microscope model JSM-5410 with Electron probe micro-analyzer (JEOL) at 30 kV.

## 1.6 H<sub>2</sub>-temperature programmed reduction (H<sub>2</sub>-TPR)

H<sub>2</sub>-TPR diagrams were obtained for ZnO-CuO/Al<sub>2</sub>O<sub>3</sub> catalyst in a microreactor loaded with previously calcined sample at 500 °C in presence of a mixture of H<sub>2</sub> and N<sub>2</sub> (5% H<sub>2</sub>) at a flow rate of 20 mL/min. The heating rate was fixed at 10 °C/min and the heating programming continued from 100 °C up to 300 °C.

## 1.7 Dispersion of the metal (s) in the catalysts

The dispersion of the metal (s) in the catalysts (metal fraction exposed) was determined by hydrogen chemisorption using a pulse-technique similar to that used by Freel<sup>[20]</sup>.

# 2 Results and discussion

## 2.1 Characterization of catalysts

### 2.1.1 XRD

The XRD patterns of the current catalysts are shown in Figure 1, which clearly exhibit the typical  $\gamma$ -phase of alumina. Table 1 presents the average particle size of various catalysts calculated by Deby-

Scherrer formula, where the catalysts prepared under the effect of ultrasonic irradiation exhibited the smallest crystallite size.

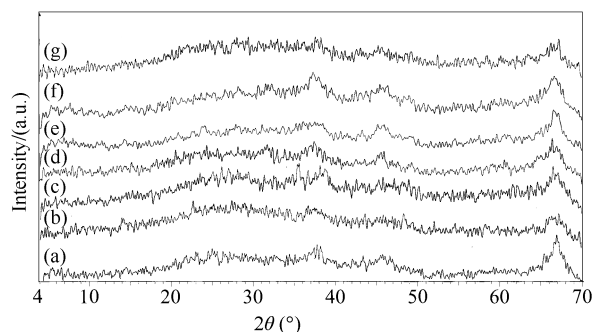


Figure 1 XRD patterns of the current catalysts (a):  $\text{Al}_2\text{O}_3$ ; (b):  $\text{CuO}/\text{Al}_2\text{O}_3$ ; (c):  $\text{CuO}/\text{Al}_2\text{O}_3(\text{U})$ ; (d):  $\text{ZnO}/\text{Al}_2\text{O}_3$ ; (e):  $\text{ZnO}/\text{Al}_2\text{O}_3(\text{U})$ ; (f):  $\text{ZnO-CuO}/\text{Al}_2\text{O}_3$ ; (g):  $\text{ZnO-CuO}/\text{Al}_2\text{O}_3(\text{U})$

### 2.1.2 BET

The specific surface area of the synthesized nanocatalysts is listed in Table 1, where the surface area of the catalysts is found to increase by

Table 1 Surface properties and metal(s) dispersion of the current alumina catalysts

Catalyst	$A_{\text{BET}}$ $/(\text{m}^2 \cdot \text{g}^{-1})$	Total pore volume $v/(\text{cm}^3 \cdot \text{g}^{-1})$	Particle size $d^a/\text{nm}$	Crystallite size $d^b/\text{nm}$	Metal (s) dispersion /%
$\text{Al}_2\text{O}_3$	203.7	0.11	8.0	12.7	–
$\text{CuO}/\text{Al}_2\text{O}_3$	177.8	0.08	9.1	9.5	45.5
$\text{CuO}/\text{Al}_2\text{O}_3(\text{U})$	246.2	0.12	6.6	7.5	52.7
$\text{ZnO}/\text{Al}_2\text{O}_3$	164.4	0.09	9.9	8.6	38.5
$\text{ZnO}/\text{Al}_2\text{O}_3(\text{U})$	244.4	0.12	6.6	6.0	45.8
$\text{ZnO-CuO}/\text{Al}_2\text{O}_3$	149.7	0.07	10.8	10.3	48.8
$\text{ZnO-CuO}/\text{Al}_2\text{O}_3(\text{U})$	230.7	0.11	7.0	7.8	56.2

<sup>a</sup>determined by BET area; <sup>b</sup>determined by XRD results

### 2.1.3 SEM

Figure 2 shows the SEM photographs for the  $\text{CuO}/\text{Al}_2\text{O}_3$ ,  $\text{ZnO}/\text{Al}_2\text{O}_3$  and  $\text{ZnO-CuO}/\text{Al}_2\text{O}_3$  catalysts prepared via precipitation of the nitrates of Cu, Zn and co-precipitation of Cu and Zn nitrates. Evidently, the ultrasonicated catalysts are formed of much smaller nano-particles than those prepared without ultrasonication. Agglomeration is found to be more significant in case of preparing the bimetallic oxide catalyst than the monometallic oxide one.

### 2.1.4 $\text{H}_2$ -TPR

Figure 3 depicts the  $\text{H}_2$ -TPR profiles obtained for the  $\text{ZnO-CuO}/\text{Al}_2\text{O}_3$  catalyst, before and after ultrasonication. Evidently, ultrasonication has caused CuO to be reduced at lower temperatures than without sonication which may contribute to increasing the activity of the ultrasonicated catalyst for DME

ultrasonication due to its decreasing particle size. These results indicate that applying irradiation of ultrasonic to the catalysts increases their surface area as well as the total pore volume.

Hence, ultrasonic irradiation applied to a catalyst during its preparation gives it higher porosity.

The theoretical particle sizes have been calculated from surface area, assuming spherical particles according to the following equation<sup>[21]</sup>:

$$d_{\text{BET}} = 6000 / \rho \times A \quad (1)$$

Where  $d_{\text{BET}}$  is the equivalent particle diameter (nm),  $\rho$  is the density of the material ( $\text{g}/\text{cm}^3$ ), and  $A$  is the specific surface area ( $\text{m}^2/\text{g}$ ). It can be observed from Table 1 that the equivalent particle diameter decreased with the ultrasound irradiation. This observation confirms the positive effect of ultrasound irradiation in decreasing the particle size. As a result, it can be seen that the particle size of ultrasonicated catalysts  $\text{CuO}/\text{Al}_2\text{O}_3(\text{U})$ ,  $\text{ZnO}/\text{Al}_2\text{O}_3(\text{U})$  and  $\text{ZnO-CuO}/\text{Al}_2\text{O}_3(\text{U})$  are smaller than those of non-ultrasonicated versions.

production from methanol where the dehydrogenative activity plays an important role in the reaction mechanism. Figure 3 shows two reduction peaks at about 220 and 250 °C, which corresponding to reduction of CuO and  $\text{Cu}_2\text{O}$ , respectively. Figure 3 also shows that the  $\text{H}_2$ -TPR profile for CuO reduction in case of ultrasonicated catalyst is smaller than before ultrasonication which indicates that CuO has been highly dispersed which is in accordance with increasing the catalytic activity (Table 1 & Figure 6). It is to be noted that ZnO cannot be reduced under the given conditions. Since reduction temperature of ZnO to metallic is higher than 650 °C, no ZnO reduction peaks observed in this study. In this case, zinc can improve the dispersion of CuO and promote the reducibility of CuO<sup>[22~25]</sup>.

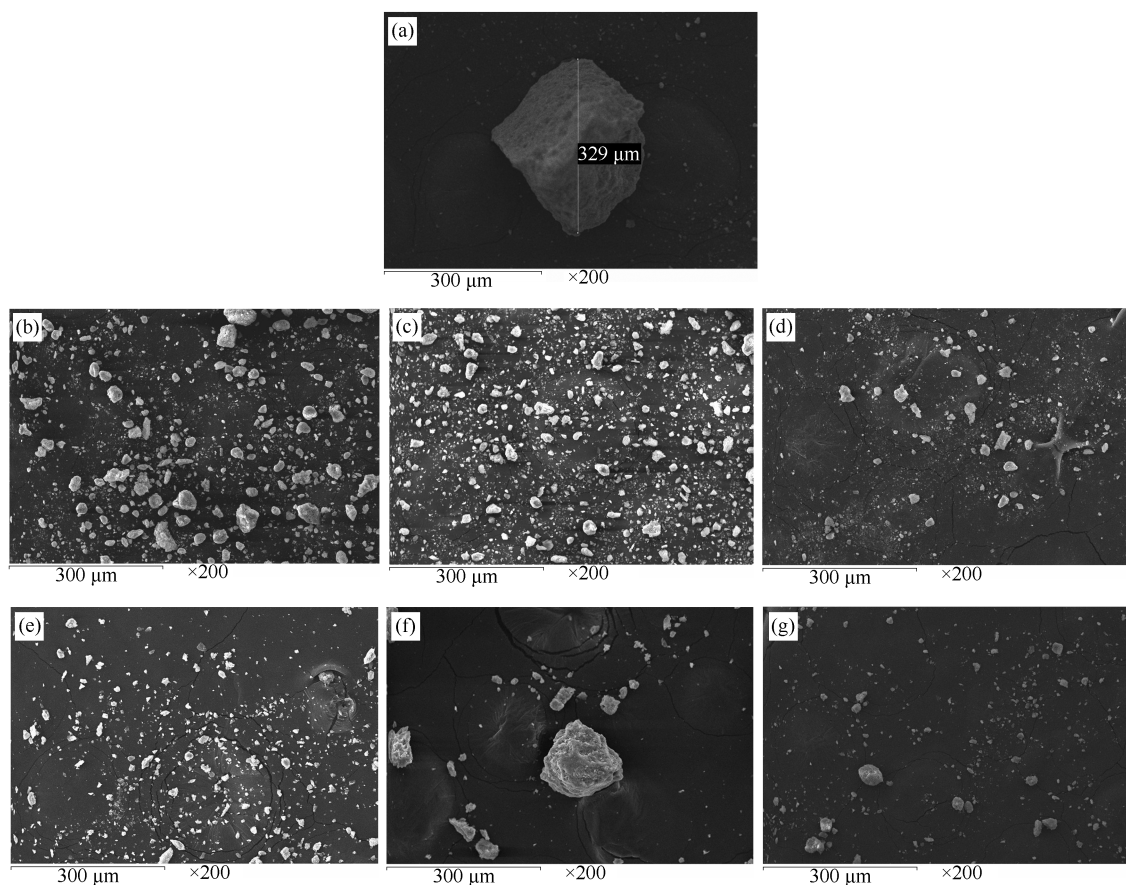


Figure 2 SEM photographs of alumina catalysts

(a) :  $\gamma\text{-Al}_2\text{O}_3$ ; (b) :  $\text{CuO}/\gamma\text{-Al}_2\text{O}_3$ ; (c) :  $\text{CuO}/\gamma\text{-Al}_2\text{O}_3(\text{U})$ ; (d) :  $\text{ZnO}/\gamma\text{-Al}_2\text{O}_3$ ; (e) :  $\text{ZnO}/\gamma\text{-Al}_2\text{O}_3(\text{U})$ ;  
(f) :  $\text{ZnO-CuO}/\gamma\text{-Al}_2\text{O}_3$ ; (g) :  $\text{ZnO-CuO}/\gamma\text{-Al}_2\text{O}_3(\text{U})$

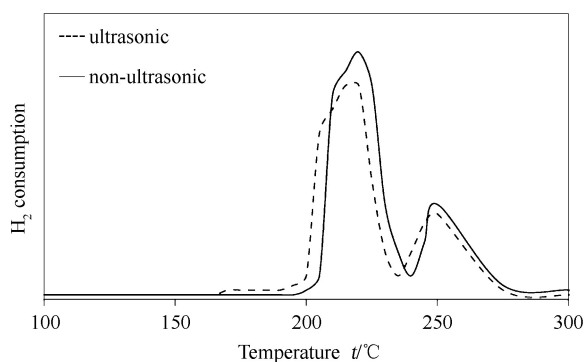


Figure 3  $\text{H}_2$ -TPR profiles of ultrasonicated  $\text{ZnO-CuO}/\text{Al}_2\text{O}_3$  catalysts

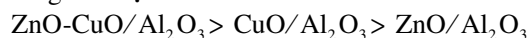
### 2.1.5 $\text{NH}_3$ -TPD

Figure 4 gives two  $\text{NH}_3$ -TPD profiles for the  $\text{ZnO-CuO}/\text{Al}_2\text{O}_3$  catalyst before and after ultrasonication. Both profiles include a major peak in the temperature range  $100 \sim 275^\circ\text{C}$  with maximum at  $\sim 200^\circ\text{C}$ . This low temperature peak corresponds to the desorption enthalpy of  $\text{NH}_3$  from the weak acid sites in the current catalyst. Also another peak with low intensity appears at temperatures between 275 and

$375^\circ\text{C}$  with maximum at  $\sim 325^\circ\text{C}$  corresponding to ammonia desorption enthalpy from the strong acid sites. Evidently, the ultrasonicated (dashed curve) obtained for the low temperature peak encounters a shift towards higher temperature indicating an increase of the acid strength of these acid sites. Moreover, the higher temperature peak has also encountered some increase of its height indicating no change of acid strength but show some increase of the number of strong acid sites.

### 2.1.6 Metal active dispersion

Metal active dispersion is the ratio of metal exposes to surface in comparison to total metal in the catalyst. Table 1 shows that effect ultrasonic can increase metal dispersion that is compared to non-ultrasonic catalysts. Dispersion can be arranged in the following order:



$\text{CuO}$  acquire higher dispersion than  $\text{ZnO}$  whether before or after sonication. Combining  $\text{ZnO}$  with  $\text{CuO}$  is found to increase the dispersion of the bimetal. In all cases ultrasonication increases the metals dispersion. Ultrasonic has very high energy that

causes collision between particle more intensive and results on the much smaller particle size<sup>[17]</sup>.

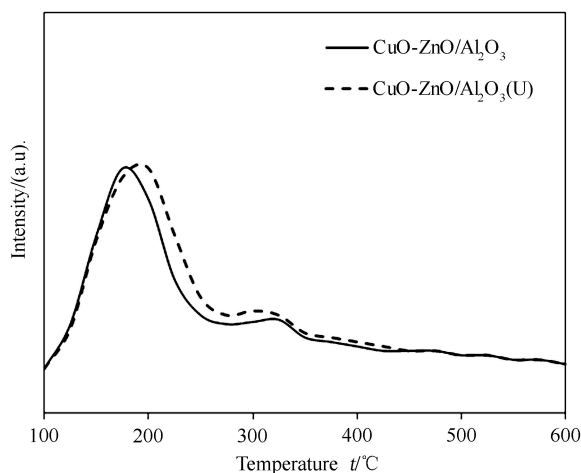


Figure 4  $\text{NH}_3$ -TPD profiles for  $\text{ZnO-CuO}/\text{Al}_2\text{O}_3$  catalysts

## 2.2 Catalytic activity, selectivity and stability

Figure 5 illustrates the promotional effectiveness of 6%  $\text{ZnO}/\text{Al}_2\text{O}_3$ , 6%  $\text{CuO}/\text{Al}_2\text{O}_3$  and their mixture 3%  $\text{ZnO}$ -3%  $\text{CuO}/\text{Al}_2\text{O}_3$  as catalysts for the methanol dehydration reaction at temperatures between 200 ~ 400 °C. Figure 5 shows that the activities of the current catalysts in the reaction temperature range 225 ~ 350 °C can be arranged in the order:

$$\text{ZnO-CuO}/\text{Al}_2\text{O}_3 > \text{CuO}/\text{Al}_2\text{O}_3 > \text{ZnO}/\text{Al}_2\text{O}_3 > \text{Al}_2\text{O}_3$$

The data indicate that  $\text{ZnO}$  and  $\text{CuO}$  act as mutual promoters for  $\text{Al}_2\text{O}_3$ . These promotional effects can be principally attributed to enhancing the acidity (acid sites number and strength)<sup>[26]</sup>. It is observed that the higher the activity of a catalyst at lower temperatures, the faster the drop of this activity at higher temperature. For instance,  $\text{ZnO-CuO}/\text{Al}_2\text{O}_3$  is the most active, so it shows an activity drop at 325 °C, whereas  $\text{CuO}/\text{Al}_2\text{O}_3$  is less active than  $\text{ZnO-CuO}/\text{Al}_2\text{O}_3$  but its activity declines at 375 °C. Even though  $\text{ZnO}/\text{Al}_2\text{O}_3$  is the least active among the current catalysts and continues its DME enhancement up to as high as 400 °C where on this catalyst, DME is the only product obtained, i. e. no olefinic hydrocarbon by-product was formed (in Figure 7).

The surface investigation data obtained using the 6%  $\text{CuO}$ , 6%  $\text{ZnO}$  and 3%  $\text{ZnO}$  + 3%  $\text{CuO}/\text{Al}_2\text{O}_3$  catalysts are given in Table 1. Evidently, the unloaded  $\text{Al}_2\text{O}_3$  acquires a surface area and total pore volume of 203.7  $\text{m}^2/\text{g}$  and 0.11  $\text{cm}^3/\text{g}$ , respectively; whereas, the  $\text{CuO}/\text{Al}_2\text{O}_3$  catalyst acquires a lower surface area (177.8  $\text{m}^2/\text{g}$ ) and lower pore volume (0.08  $\text{cm}^3/\text{g}$ ) due to some pore

filling in  $\text{Al}_2\text{O}_3$  with the metal.

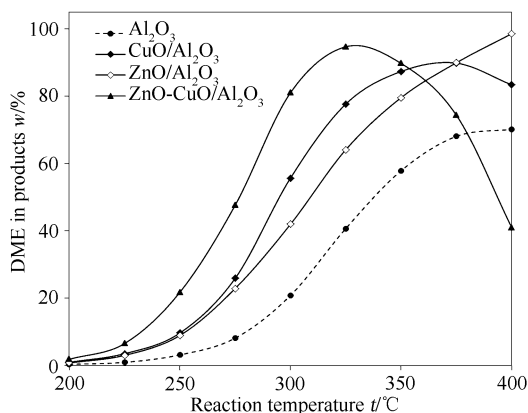


Figure 5 DME in products using alumina catalysts

Ultrasonication of the  $\text{CuO}/\text{Al}_2\text{O}_3$  catalyst is found to increase the surface area and pore volume to 246.2  $\text{m}^2/\text{g}$  and 0.12  $\text{cm}^3/\text{g}$ , respectively, indicating that ultrasonication has loosened some already present agglomerates of the catalytic particles. Figure 6 shows that using the  $\text{CuO}/\text{Al}_2\text{O}_3(\text{U})$  ultrasonicated catalyst, the increase of temperature from 200 up to 300 °C has increased DME almost linearly to reach 90% at 300 °C, beyond which DME increases slowly to 94.5% at 375 °C. It may be assumed that this moderate increase of surface area and pore volume associated with an increase of catalytic activity can be attributed to an increase of the density of acid sites of the  $\text{CuO}/\text{Al}_2\text{O}_3$  particles in the catalytic bed inside the reaction.

Also, the treatment of the  $\text{ZnO}/\text{Al}_2\text{O}_3$  catalyst via applying ultrasonication, producing ( $\text{ZnO}/\text{Al}_2\text{O}_3(\text{U})$ ), has increased the surface area and pore volume from 164.4  $\text{m}^2/\text{g}$ , respectively, and 0.09  $\text{cm}^3/\text{g}$  to 244.4  $\text{m}^2/\text{g}$  and 0.12  $\text{cm}^3/\text{g}$ , respectively. This increase of surface area and pore volume, associated with an increase of catalytic activity (in Figure 6) by virtue of ultrasonication can be said to operate in accordance with optimized catalytic bed packing. Nevertheless, the ultrasonication effectiveness on the catalytic reaction does not exhibit deviated behaviors of the  $\text{CuO}$  and  $\text{ZnO}$  sites relative to the catalytic sites of the  $\text{Al}_2\text{O}_3$  support. In Figure 6, using the  $\text{ZnO}$  promoted catalyst, DME is increased with temperature to attain a maximum of 88.0% at 325 °C, beyond which it declines via a further increase of temperature to attain 72.0% at 400 °C due to side product formation (in Figure 7).

The ultrasonicated  $\text{ZnO-CuO}/\text{Al}_2\text{O}_3$  is more active than the non-ultrasonicated version in the temperature range 100 ~ 325 °C. However, at higher temperatures

(325 ~400 °C) a strong deviation takes place, where the ultrasonicated catalyst is steadily activated, but the non-ultrasonicated one suffers a significant drop of catalytic

activity. This can be considered a valuable advantage for impeding the deteriorative side reaction producing olefins instead of DME.

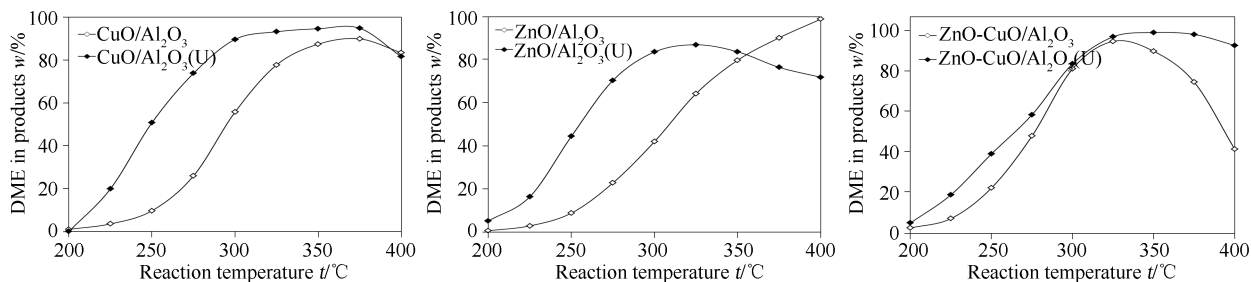


Figure 6 Effect of ultrasonication on DME formation using alumina catalysts

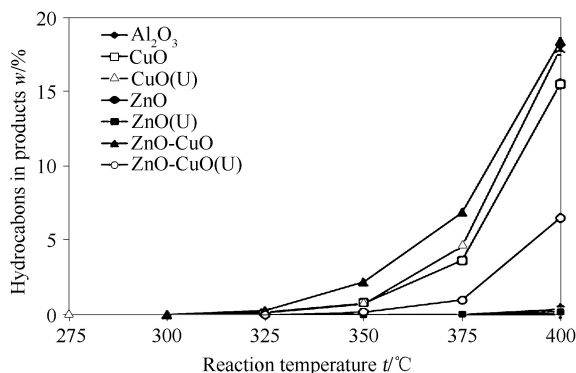


Figure 7 Hydrocarbons in products using alumina catalysts

In case of the bimetallic ZnO-CuO/Al<sub>2</sub>O<sub>3</sub> catalyst, the surface area has significantly increased from 149.7 to 230.7 m<sup>2</sup>/g and the pore volume also increased from 0.07 to 0.11 cm<sup>3</sup>/g using ultrasonication. Such correlation indicates that ultrasonication has increased these surface characteristics in case of the ZnO-CuO/Al<sub>2</sub>O<sub>3</sub> catalysts but decreased them in case of the monometallic CuO/Al<sub>2</sub>O<sub>3</sub> catalyst. However, for all catalysts the ultrasonication treatment improved the catalytic activities for DME production due to increasing the acid sites number and strength as well as to increasing the surface area and pore volume in addition to decreasing the nanoparticle size of the catalysts (in Figure 4 & Table 1) as noticed in acquiring increased reducibility of the metal oxides (in Figure 3).

The selectivity for producing DME and hydrocarbons in the reaction product at a relatively high reaction temperature (400 °C) is shown in Figure 8 for the current catalysts. The highest selectivity for DME is 99.7% using the ZnO/Al<sub>2</sub>O<sub>3</sub> catalyst either using or not using ultrasonication. However, for CuO/Al<sub>2</sub>O<sub>3</sub>, DME is somewhat less selective after ultrasonication (84.3% vs. 81.5%), whereas the selectivity to hydrocarbons is somewhat

higher after ultrasonication (18.5% vs. 15.7%). On the other hand, the bimetallic ZnO-CuO/Al<sub>2</sub>O<sub>3</sub> catalyst exhibits a great improvement for DME selectivity after ultrasonication (93.4% vs. 69.0%) and hydrocarbon selectivity of 6.6% vs. 31.0%. Here, the metals dispersion has been improved via combining both metals in presence of ultrasonication irradiation in addition to increasing the acid site strength (in Figure 4).

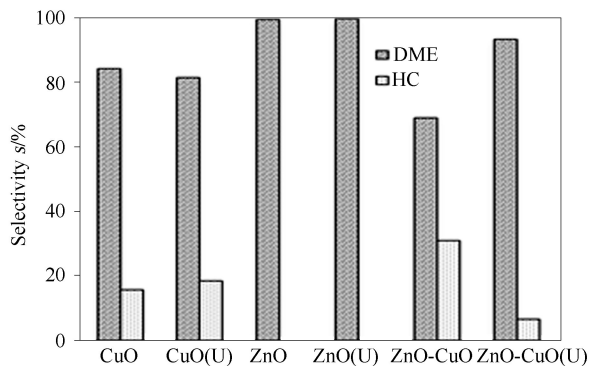


Figure 8 Effect of ultrasonication (U) on DME and HC selectivities using current catalysts at 400 °C

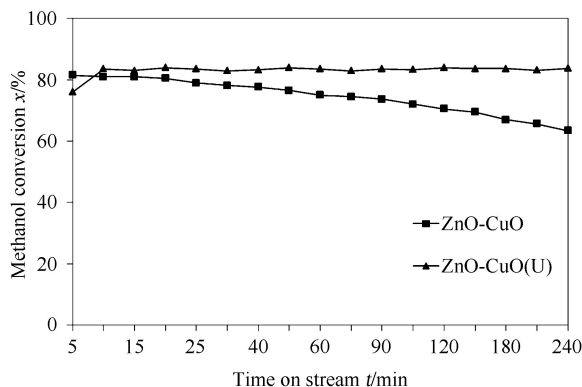


Figure 9 Effect of time on methanol conversion using ZnO-CuO/Al<sub>2</sub>O<sub>3</sub> catalysts at 300 °C

Figure 9 shows that the stability of ZnO-CuO/

Al<sub>2</sub>O<sub>3</sub> catalyst, as a function of time-on-stream, has been significantly improved via ultrasonication such that DME production continued without any drop in activity up to 240 min. This can be attributed to enhancing the dispersion of the metal oxide on the alumina support by ultrasonication<sup>[27]</sup>.

### 3 Conclusions

The overall effect of ultrasonication in improving

the catalytic activity and selectivity for DME using the CuO/Al<sub>2</sub>O<sub>3</sub>, ZnO/Al<sub>2</sub>O<sub>3</sub> and ZnO-CuO/Al<sub>2</sub>O<sub>3</sub> catalysts which can be attributed to: increasing the acid sites number and strength, increasing the surface area and pore volume, decreasing the nanoparticle size of the catalysts, activating the reducibility of the metallic components, increasing the catalytic stability and increasing the metal(s) dispersion.

### References

- [1] FLEISCH T H, BASU A, GRADASSI M J, MASIN J G. Dimethyl ether: A fuel for the 21st century[J]. *Stud Surf Sci Catal*, 1997, **107**: 117-125.
- [2] SEMELSBERGER T A, BORUP R L, GREENE H L. Dimethyl ether (DME) as an alternative fuel[J]. *J Power Sources*, 2006, **156**(2): 497-511.
- [3] VISHWANATHAN V, JUN K W, KIM J W, ROH H S. Vapour phase dehydration of crude methanol to dimethyl ether over Na-modified H-ZSM-5 catalysts[J]. *Appl Catal A: Gen*, 2004, **276**(1/2): 251-256.
- [4] CAI G Y, LIU Z M, SHI R M, HE C Q, YANG L X, SUN C L, CHANG Y J. Light alkenes from syngas via dimethyl ether[J]. *Appl Catal A: Gen*, 1995, **125**(1): 29-38.
- [5] XU M T, GOODMAN D W, BHATTACHARYYA A. Catalytic dehydration of methanol to dimethyl ether (DME) over Pd/Cab-O-Sil catalysts[J]. *Appl Catal A: Gen*, 1997, **149**: 303-309.
- [6] KIM S D, BAEK S C, LEE Y J, JUN K W, KIM M J, YOO I S. Effect of  $\gamma$ -alumina content on catalytic performance of modified ZSM-5 for dehydration of crude methanol to dimethyl ether[J]. *Appl Catal A: Gen*, 2006, **309**(1): 139-143.
- [7] VISHWANATHAN V, ROH H S, KIM J W, JUN K W. Surface properties and catalytic activity of TiO<sub>2</sub>-ZrO<sub>2</sub> mixed oxides in dehydration of methanol to dimethyl ether[J]. *Catal Lett*, 2004, **96**(1/2): 23-28.
- [8] FEI J H, HOU Z Y, ZHU B, LOU H, ZHENG X M. Synthesis of dimethyl ether (DME) on modified HY zeolite and modified HY zeolite-supported Cu-Mn-Zn catalysts[J]. *Appl Catal A: Gen*, 2006, **304**: 49-54.
- [9] YARIPOUR F, BAGHAEI F, SCHMIDT I, PERREGAARD J. Catalytic dehydration of methanol to dimethyl ether (DME) over solid-acid catalysts[J]. *Catal Commun*, 2005, **147**(6): 147-152.
- [10] KIM S M, LEE Y J, BAE J W, POTDAR H S, JUN K W. Synthesis and characterization of a highly active alumina catalyst for methanol dehydration to dimethyl ether[J]. *Appl Catal A: Gen*, 2008, **348**(1): 113-120.
- [11] ZHANG Y L, SUN Q, DENG J F, WU D. A high activity Cu/ZnO/Al<sub>2</sub>O<sub>3</sub> catalyst for methanol synthesis: Preparation and catalytic properties[J]. *Appl Catal A: Gen*, 1997, **158**(1/2): 105-120.
- [12] REUBROYCHAROEN P, VITIDSANT T, YONEYAMA Y, TSUBAKI N. Development of a new low-temperature methanol synthesis process [J]. *Catal Today*, 2004, **89**(4): 447-454.
- [13] MAO D S, YANG W M, XIA J C, ZHANG B, SONG Q Y, CHEN Q L. Highly effective hybrid catalyst for the direct synthesis of dimethyl ether from syngas with magnesium oxide-modified HZSM-5 as a dehydration component[J]. *J Catal*, 2005, **230**(1): 140-149.
- [14] BALTES C, VUKOJEVIC S, SCHÜTH F. Correlations between synthesis, precursor, and catalyst structure and activity of a large set of CuO/ZnO/Al<sub>2</sub>O<sub>3</sub> catalysts for methanol synthesis[J]. *J Catal*, 2008, **258**(2): 334-344.
- [15] BEHRENS M. Meso- and nano-structuring of industrial Cu/ZnO/Al<sub>2</sub>O<sub>3</sub> catalysts[J]. *J Catal*, 2009, **267**(1): 24-29.
- [16] YANG G H, TSUBAKI N, SHAMOTO J, YONEYAMA Y, ZHANG Y. Confinement effect and synergistic function of H-ZSM-5/Cu-ZnO-Al<sub>2</sub>O<sub>3</sub> capsule catalyst for one-step controlled synthesis[J]. *J Am Chem Soc*, 2010, **132**(23): 8129-8136.
- [17] ABOUL-FOTOUH S M K. Effect of ultrasonic irradiation and/or halogenation on the catalytic performance of  $\gamma$ -Al<sub>2</sub>O<sub>3</sub> for methanol dehydration to dimethyl ether[J]. *J Fuel Chem Technol*, 2013, **41**(9): 1077-1084.
- [18] ABOUL-GHEIT A K. Acid site strength distribution in mordenites by differential scanning calorimetry[J]. *J Catal*, 1988, **113**(2): 490-496.
- [19] ABOUL-GHEIT A K. Effect of decationation and dealumination of zeolite Y on its acidity as assessed by ammonia desorption measured by differential scanning calorimetry (DSC)[J]. *Thermochim Acta*, 1991, **191**(2): 233-240.
- [20] FREEL J. Chemisorption on supported platinum; I. Evaluation of a pulse method[J]. *J Catal*, 1972, **25**(1): 139-148.
- [21] REZAEI M, ALAVI S M, SAHEBDELFAH S, YAN Z F. Tetragonal nanocrystalline zirconia powder with high surface area and mesoporous structure[J]. *Powder Technol*, 2006, **168**(2): 59-63.
- [22] KHOSHBIN R, HAGHIGHI M. Direct syngas to DME as a clean fuel: The beneficial use of ultrasound for the preparation of CuO-ZnO-Al<sub>2</sub>O<sub>3</sub>/HZSM-5 nanocatalyst[J]. *Chem Eng Res Des*, 2013, **91**(6): 1111-1122.
- [23] XIA S, NIE R, LU X, WANG L, CHEN P, HOU Z. Hydrogenolysis of glycerol over Cu<sub>0.4</sub>/Zn<sub>5.6-x</sub>Mg<sub>x</sub>Al<sub>2</sub>O<sub>8.6</sub> catalysts: The role of basicity and hydrogenation spillover[J]. *J Catal*, 2012, **296**: 1-11.
- [24] NIE R, LEI H, PAN S, WANG L, FEI J, HOU Z. Core-shell structured CuO-ZnO@H-ZSM-5 catalysts for CO hydrogenation to dimethyl ether[J]. *Fuel*, 2012, **96**: 419-425.
- [25] FEI J, YANG M, HOU Z, ZHENG X. Effect of the addition of manganese and zinc on the properties of copper-based catalyst for the synthesis of syngas to dimethyl ether[J]. *Energy Fuels*, 2004, **18**(5): 1584-1587.
- [26] YANG M, MEN Y, LI S, CHEN G. Hydrogen production by steam reforming of dimethyl ether over ZnO-Al<sub>2</sub>O<sub>3</sub> bi-functional catalyst[J]. *Int J Hydrog Energy*, 2012, **37**(10): 8360-8369.
- [27] NASIKIN M, WAHID A. Effect of ultrasonic during preparation on Cu-based catalyst performance for hydrogenation of CO, to methanol[J]. *AJChE*, 2005, **5**(2): 111-115.